Synthesis of Germanium Nanocrystals in High Temperature Supercritical Fluid Solvents

ARTICLE *in* NANO LETTERS · APRIL 2004

Impact Factor: 13.59 · DOI: 10.1021/nl049831j

NANO LETTERS

2004
Vol. 4, No. 5
969−974

Synthesis of Germanium Nanocrystals in High Temperature Supercritical Fluid Solvents

Xianmao Lu, Kirk J. Ziegler, Ali Ghezelbash, Keith P. Johnston,* and Brian A. Korgel*

Department of Chemical Engineering, Texas Materials Institute, and Center for Nano- and Molecular Science and Technology, The University of Texas at Austin, Austin, Texas 78712

Received January 28, 2004; Revised Manuscript Received February 24, 2004

ABSTRACT

Crystalline germanium (Ge) nanocrystals were synthesized by arrested precipitation in supercritical hexane and octanol at 400∼550 °C and 20.7 MPa in a continuous flow reactor. Two Ge precursors were explored, diphenylgermane (DPG) and tetraethylgermane (TEG), which undergo thermolysis to crystalline Ge under these conditions. Octanol is added to control particle growth, which appears to serve as a capping ligand that binds to the particle surface through an alkoxide linkage. The nanocrystals were characterized by high-resolution transmission electron microscopy (HRTEM), energy-dispersive X-ray spectroscopy (EDS), FTIR spectroscopy, and X-ray diffraction (XRD). The average nanocrystal diameter could be changed over a wide range, from ∼2 nm to ∼70 nm, by varying the reaction temperature and precursor concentration. Relatively size-monodisperse nanocrystals could be produced, with standard deviations about the mean diameter as low as ∼10%. UV−visible absorbance and photoluminescence (PL) spectra of Ge nanocrystals in the 3 to 4 nm diameter size range exhibit optical absorbance and PL spectra blue-shifted by approximately 1.7 eV relative to the band gap of bulk Ge, with quantum yields up to 6.6%.

A variety of metal and semiconductor nanocrystal materials can be produced by solution-phase arrested precipitation.[1] In this process, molecular precursors are degraded either by reduction/oxidation or thermolysis in the presence of capping ligands that bind to nucleating and growing particles and inhibit growth, and also provide redispersibility in compatible solvents. Interest in these "free-standing" nanocrystals derives from their unique size-tunable physical properties, relative chemical stability, redispersibility in various solvents, and chemically functionalizable surfaces. Group IV nanocrystals, such as Si and Ge, have been particularly challenging to synthesize by solution-phase methods, primarily due to their strong covalent bonding and the need for high temperatures to promote crystallization. Although a few research groups have reported crystalline Ge nanocrystal synthesis in solution at temperatures lower than 300 °C,[2−4] chemical vapor deposition of Ge typically requires temperatures exceeding 415 °C to crystallize the films[5] without the aid of a catalyst, such as gold.[6] Since this temperature range exceeds the boiling point of conventional solvents under ambient conditions, we have been exploring high-temperature pressurized solvents as reaction media for nanostructure synthesis.[7−13] For example, these solvents—called supercritical fluids (SCF) when the temperature and pressure exceed the critical temperature and pressure—have been vital to the formation of Si[7,14,15] nanocrystals and Si,[9,10] Ge,[11,12] and GaAs[13] nanowires. Here, we report the arrested precipitation synthesis of Ge nanocrystals utilizing a SCF as a solvent in a high-pressure high-temperature continuous flow reactor.

Ge nanocrystals were synthesized by thermally degrading either tetraethylgermane (TEG) or diphenylgermane (DPG), in the presence of octanol at temperatures ranging from 400 °C to 550 °C at 20.7 MPa. The reactions were carried out using a flow reactor system like that described in detail by Lu et al.[10] The precursor solutions were either TEG (Gelest) in a 1:3 (volume ratio) mixture of octanol (T_c = 385 °C, P_c = 3.45 MPa) and hexane (T_c = 235 °C, P_c = 3.0 MPa), or DPG (Gelest) in pure octanol. Table 1 lists the TEG and DPG concentrations studied. The solutions were prepared in a nitrogen-filled glovebox using solvents that were purchased anhydrous and packaged under nitrogen (Aldrich Chemical Co.). The reactants are fed from a variable volume stainless steel cylinder with an HPLC pump (to control the reactor pressure and flow rate) into a 2 mL (0.5 cm i.d., 2.0 cm o.d., and 12.5 cm long) high-pressure titanium grade-2 cell with both ends connected to 1/16 in. o.d. and 0.03 in. i.d. stainless steel high-pressure tubing via titanium grade-2 LM-6 HIP reducers (High Pressure Equipment). The inlet stream was preheated to ∼300 °C prior to entering the

* Corresponding authors: (Johnston) (T) 512-471-4617; (F) 512-471-7060; (E-mail) kpj@che.utexas.edu. (Korgel) (T) 512-471-5633; (F) 512-471-7060; (E-mail) korgel@mail.che.utexas.edu.

10.1021/nl049831j CCC: $27.50
Published on Web 04/07/2004

Table 1. Summary of the Mean Diameter $\overline{d_p}$, and Standard Deviation about the Mean Diameter σ, of Ge Nanocrystals Synthesized at Various Temperatures, Residence Times τ, and Ge Precursor Concentrations

reactor	precursor (mM)	T (°C)	τ (sec)	N^a	$\overline{d_p}$ (nm)	σ (%)
flow	[TEG] = 62.5	450	300	86	4.2	10
flow	[TEG] = 62.5	550	300	165	4.8	19
flow	[TEG] = 25.0	450	300	148	2.0	20
batch	[TEG] = 62.5	450	300	71	3.5	54
flow	[DPG] = 100.0	400	20	326	71.4	28
flow	[DPG] = 50.0	400	20	474	49.8	23
flow	[DPG] = 25.0	400	20	217	3.8	24
flow	[DPG] = 12.5	400	20	125	3.1	31
batch	[DPG] = 25.0	400	20	162	6.5	52

[a] N is the number of Ge nanocrystals counted for each sample to construct the histograms used to determine the $\overline{d_p}$ and σ.

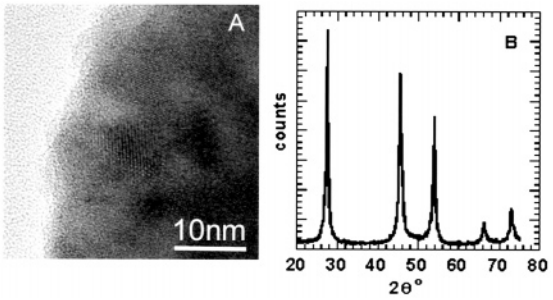

Figure 1. (A) TEM image of polycrystalline Ge formed from TEG pyrolysis in hexane at 450 °C and 20.7 MPa. (B) The XRD pattern indexes to diamond cubic Ge and indicates from the peak breadth a crystal domain size of ~60 nm.

reactor. An SS-4R3A back-pressure regulator (Swagelok) connected after the reaction cell and a digital pressure gauge (Stratford) between the preheater tubing and the cell maintained the pressure at 20.7 MPa. The product is collected as it exits the back-pressure regulator of the reactor.

After collection from the reactor, the Ge nanocrystals were purified for characterization. The sample was first dried on a rotary evaporator for 2 h and then vacuum distilled overnight to remove the light organic and oily byproducts, resulting in a weight loss of more than 95%. The Ge nanocrystals were then redispersed in 0.1 mL chloroform and precipitated with 10 mL ethanol for further purification. The precipitated nanocrystals were collected by centrifugation at 10 000 rpm for 5 min. This step yields a dry residue of nanocrystals that can be redispersed in various organic solvents, including chloroform and hexane. The nanocrystals were characterized by transmission electron microscopy (TEM), X-ray diffraction (XRD), Fourier transform infrared spectroscopy (FTIR), UV−visible absorbance and photoluminescence emission (PL), and excitation (PLE) spectroscopy.

Decomposition of TEG in pure hexane at 450 °C and 20.7 MPa produces micrometer-size bulk polycrystalline Ge particulates. Figure 1 shows a representative TEM image and XRD pattern from the material produced. Similar results are obtained for DPG composition in pure hexane. In contrast, when octanol is added to the reaction mixture, much smaller,

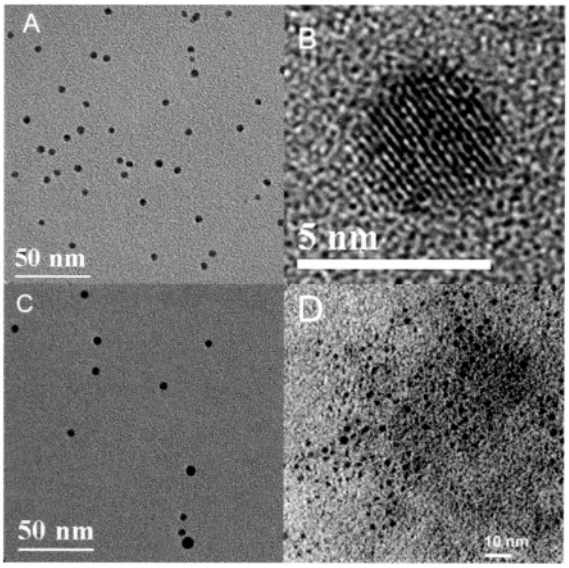

Figure 2. TEM images of octanol-stabilized Ge nanocrystals synthesized by TEG thermolysis in 1:3 v/v octanol/hexane with a reactor residence time of τ = 5 min: (A) T = 450 °C, [TEG] = 62.5 mM, $\overline{d_p}$ = 4.2 ± 0.42 nm; (B) HRTEM image of a Ge nanocrystal from the sample in (A); (C) T = 550 °C, [TEG] = 62.5 mM, $\overline{d_p}$ = 4.8 ± 0.93 nm; (D) T = 450 °C, [TEG] = 25.0 mM, $\overline{d_p}$ = 2.0 ± 0.40 nm.

nanometer-size Ge nanocrystals are obtained. Figure 2 shows TEM images[16] of Ge nanocrystals made from TEG in the presence of octanol at varying reaction temperature and TEG concentration. Of the conditions explored, the nanocrystals synthesized at [TEG] = 62.5 mM and 450 °C had the narrowest size distribution, with an average diameter of 4.2±0.4 nm. The HRTEM image in Figure 2B shows the internal crystallinity for one Ge nanocrystal of the sample imaged in Figure 2A. The particle appears to consist of a single crystal domain and exhibits a 0.20 nm d spacing corresponding to the {220} lattice spacing of diamond cubic Ge. An increase in reaction temperature to 550 °C at this TEG concentration did not significantly increase the nanocrystal diameter, but did increase the size distribution with $\overline{d_p}$ = 4.8±0.93 nm (Figure 2C). The standard deviation about the mean diameter of ±19% is nearly twice as broad as that obtained at 450 °C (±10%). The TEG concentration, however, does have a significant influence on the particle diameter. Ge nanocrystals produced at 450 °C at lower TEG concentration, with [TEG] = 25.0 mM (Figure 2D), were much smaller, with particle diameters of 2.0±0.40 nm.

Ge nanocrystals could also be synthesized using DPG as the reactant. The particle size, however, was more difficult to limit than when TEG was used. Nanometer-size particles could be obtained only when pure octanol was used as the solvent, with slightly lower reaction temperature (400 °C) and shorter residence time (20 s). Even at these lower reaction temperatures, residence times on the order of minutes yielded bulk polycrystalline Ge. The greater DPG reactivity provided access to a wider range of nanocrystal sizes. With relatively small changes in DPG concentration, nanocrystals could be formed with diameters as large as ~70 nm or as small as ~3 nm at the same reaction temperature.

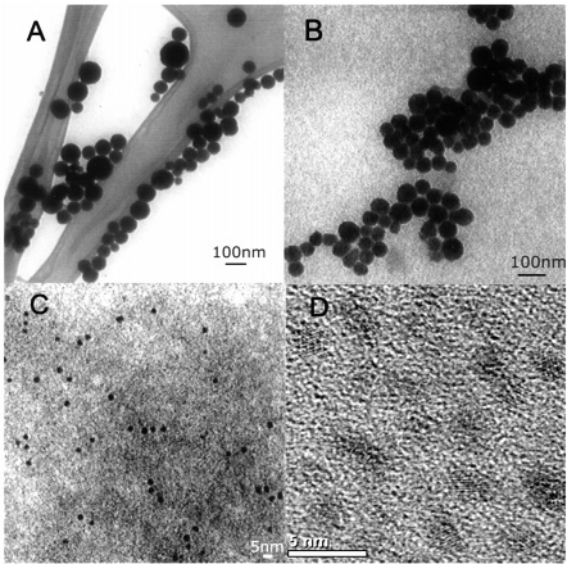

Figure 3. TEM images of Ge nanocrystals synthesized in pure octanol at 400 °C, 20.7 MPa, and a reactor residence time of 20 s: (A) [DPG] = 100 mM, $\overline{d_p}$ = 71.4 ± 19.8 nm; (B) [DPG] = 50 mM, $\overline{d_p}$ = 49.8±11.5 nm; (C) [DPG] = 25 mM, $\overline{d_p}$ = 3.8 ± 0.9 nm; (D) [DPG] = 12.5 mM, $\overline{d_p}$ = 3.1±0.9 nm.

Figure 3 shows Ge nanocrystals made from DPG at 400 °C in octanol at 20.7 MPa at different DPG concentrations. As summarized in Table 1, the Ge nanocrystals made from DPG exhibit somewhat broader size distributions than those formed using TEG.

We also explored Ge nanocrystal synthesis using a batch reactor setup. Batch reactions[17] were carried out for [TEG] = 62.5 mM and [DPG] = 25.0 mM (Table 1). The heat-up time was 2 min and the time at the reaction temperature was 5 min and 20 s for TEG and DPG, respectively. At 450 °C and [TEG] = 62.5 mM, the diameter of the Ge nanoparticles obtained from batch reaction was $\overline{d_p}$ = 3.5±1.9 nm, which is close to that of the particles produced in flow reactor at the same temperature and TEG concentration (4.2 nm). However, the standard deviation of the particles was much higher for the batch reaction than for the flow reaction (±54% versus ±10%). This increase in polydispersity was also observed for the batch reaction of DPG. For [DPG] = 25.0 mM at 400 °C, the diameter of the Ge particles was $\overline{d_p}$ = 6.5 nm with a standard deviation of ±52%, which is also higher than in the flow reaction (±24%). The lower polydispersity produced using the flow-through reactor setup reflects the greater temperature and pressure control compared to the batch reactor setup.

The 3 and 4 nm diameter Ge nanocrystals synthesized using DPG (12.5 mM and 25 mM, respectively) exhibited primarily single crystal domains in their TEM images. Figure 3D, for example, shows a field of crystalline Ge nanocrystals where many display the characteristic 0.2 nm *d* spacing of the {220} planes in diamond cubic Ge. Figure 4A shows a selected area electron diffraction (SAED) pattern obtained from a 4 nm diameter Ge nanocrystal, exhibiting the characteristic spot pattern of a single crystal domain and the hexagonal symmetry of the {111} lattice plane of Ge. In

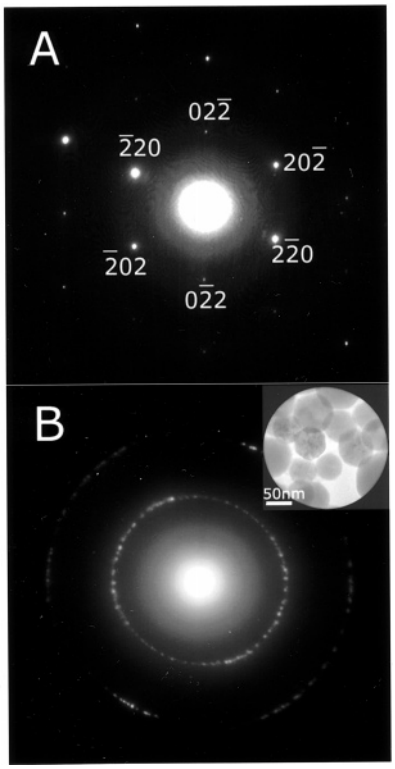

Figure 4. SAED from Ge nanocrystals synthesized by degrading DPG in octanol at 400 °C with a 20 s residence time: (A) SAED pattern obtained from an individual 4 nm diameter particle synthesized with [DPG] = 12.5 mM; (B) an SAED pattern obtained from 70 nm diameter Ge nanocrystals synthesized with [DPG] = 100 mM. The *d* spacings in (B) of the two rings (0.199 and 0.116 nm) are consistent with the reference values (0.200 nm and 0.115) for Ge {220} and {422}. The spacings were determined using Bragg's equation[18], $r = \lambda L/d$, where the radius r = 1.51 cm for the first diffraction ring and r = 2.59 cm for the second ring, the electron wavelength is λ = 0.0025079 nm for 200 keV accelerating voltage, and the camera length is L = 120 cm.

contrast, SAED patterns from Ge nanocrystals in the larger size range (50 nm to 70 nm diameter) made from higher DPG concentrations (50 mM and 70 mM, respectively) exhibit ring patterns, characteristic of internal polycrystallinity. For example, Figure 4B shows an SAED pattern obtained from the larger nanocrystals with rings corresponding to the *d* spacing between the {220} and {422} lattice planes in diamond cubic Ge. From XRD patterns obtained for the nanocrystals in this size range, the average crystalline domain size is ∼40 nm for ∼70 nm diameter nanocrystals (Figure 5B). In contrast, the crystal domain size determined from peak broadening in the XRD patterns from 3 to 4 nm diameter nanocrystals matches the particle diameter within experimental error (Figure 5B). Both XRD and elemental analysis of fields of nanocrystals by energy-dispersive X-ray spectroscopy (EDS) (Figure 5A) confirm that the nanocrystals are composed of crystalline Ge.

FTIR spectra (Thermo Mattson Infinity Gold FTIR spectrometer) of the Ge nanocrystals can provide a qualitative measure of what is coating the nanocrystal surfaces. As mentioned previously, if DPG or TEG are degraded in the absence of octanol, bulk polycrystalline Ge is produced. The octanol helps stabilize the particle size, presumably by

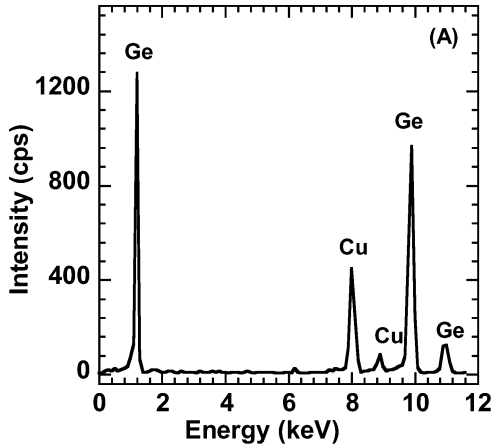

Figure 5. (A) EDS data obtained for the nanocrystals imaged by TEM in Figure 1C. The copper peaks result from the copper TEM grid used as the material support. (B) Powder XRD patterns of Ge nanocrystals made from 100 mM DPG ($\bar{d}$ = 71.4 nm) and 12.5 mM DPG ($\bar{d}$ = 3.1 nm) at 400 °C. XRD was performed using a Phillips vertical scanning diffractometer, with Cu Kα radiation (λ = 1.54 Å) and a scintillation detector. The sample was cleaned with rotary evaporator and vacuum oven and then dried as powders onto quartz slides (The Gem Dugout, State College, PA) in nitrogen glovebox. The crystal domain size was estimated from the peak width by the Scherrer formula[19] $t = 0.9\lambda/B\cos\theta_B$. The broadening of the Ge {111} reflection ($2\theta_B = 27.28°$) is $B \approx 0.21°$ (fwhm) for the 71.4 nm Ge nanoparticles, and the calculated size from Scherrer equation is 38.9 nm, which is smaller than the average diameter measured by TEM, indicating that the nanocrystals are polycrystalline. The peak broadening for the 3.1 nm Ge nanoparticles is 1.96° (fwhm), and the corresponding Scherrer diameter is 4.1 nm, which is close to the mean size determined from TEM images.

serving as a capping ligand. FTIR measurements were performed on purified Ge nanocrystals that were drop cast in air from chloroform onto intrinsic Si substrates. Three peaks appear in the FTIR spectra in Figure 6 at 2958, 2928, and 2858 cm^{-1}, characteristic of C−H stretching modes for CH_2 and CH_3 groups, indicating that hydrocarbon species coat the Ge nanocrystals. The peaks at 1468 and 1380 cm^{-1} are also consistent with the CH_3 bending vibrations. As we expect that the physisorbed and solution-phase organic species are removed in the rigorous washing steps prior to the measurement, the FTIR spectra provide a strong indication that a hydrocarbon layer is chemisorbed to the particle surface. The hydroxyl stretch for octanol (3300 cm^{-1}) is

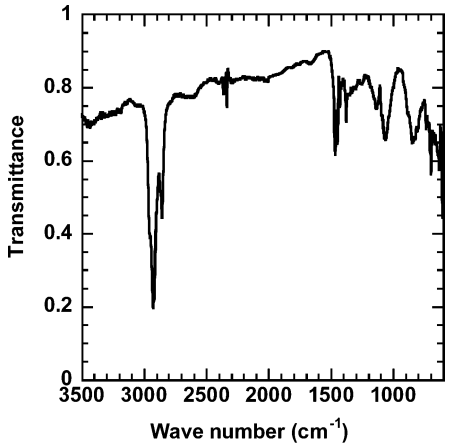

Figure 6. FTIR spectrum of Ge nanocrystals made from TEG at 400 °C on an intrinsic Si substrate.

notably absent from the spectra. The peaks at 1068 and 698 cm^{-1} could correspond to Ge−O−C species,[20−22] which would suggest covalent alkoxide bonding of the capping ligands to the Ge nanocrystal surface, although other possibilities, such as CH−O− (1100 cm^{-1}) and CH_2−O− (1050 cm^{-1}), cannot be excluded. The peak at 850 cm^{-1} (Ge−O/Ge−C stretches) indicates that the surface is also covered with either residual oxide or direct bonding between Ge and the hydrocarbon coating. But as FTIR is very sensitive to Ge−O and Ge−C stretches, the presence of these species would have to be in very small amounts. Although it does not provide definitive proof of the nature of the ligand bonding to the nanocrystal surface, the FTIR spectra indicate that hydrocarbon species coat the nanocrystal surfaces, potentially through alkoxide bonding with the Ge surface.

Ge is an indirect band gap semiconductor unsuitable for light emitting applications as a bulk material, yet can produce relatively high photoluminescence at the nanoscale.[2,23] Figure 7 shows the room-temperature UV−visible absorbance and PL/PLE spectra for 3.1 nm ([DPG] = 12.5 mM, 400 °C) and 4.2 nm ([TEG] = 62.5 mM, 450 °C) Ge nanocrystals. Bulk Ge has a band gap of 0.6 eV and according to the band structure of Ge,[2,4] the absorption coefficient of bulk Ge has distinct peaks at 550 nm (2.1 eV) and 280 nm (4.3 eV) associated with direct band transitions at *L* and *X*, respectively. Quantum confinement effects are expected to shift the energy levels in Ge nanocrystals smaller than 23 nm in diameter, since the Bohr radius for Ge is 11.5 nm.[2] The absorption edges in Figure 7 for 3.1 and 4.2 nm diameter Ge nanocrystals were significantly blue-shifted relative to the bulk Ge band gap. In fact, these absorption edges are close to those of Si nanocrystals of similar diameter,[7,14,15] as expected from predictions by several groups.[24−26] Our observed size shifts are also qualitatively consistent with those of Ge nanocrystals synthesized by Wilcoxon[2] and Heath.[4] The PL spectrum for the 4.2 nm Ge nanocrystals excited with 360 nm (3.4 eV) light shows a broad peak at 536 nm (2.3 eV), and the PLE spectrum (λ_{em} = 536 nm) shows strong absorption near 360 nm, which is responsible for the majority of light emission. The PL spectrum for the 3.1 nm Ge nanoparticles excited at 340 nm (3.7 eV) shows

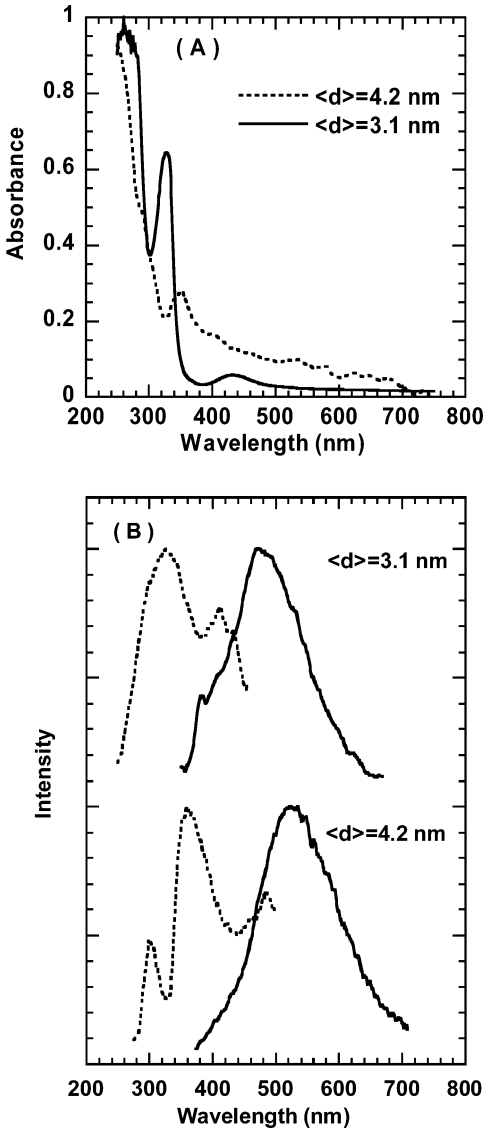

Figure 7. Room-temperature UV−visible (A) absorbance and (B) PL (solid lines, excitation wavelength λ_{ex} = 340 nm for $\overline{d_p}$ = 3.1±0.9 nm particles and λ_{ex} = 360 nm for $\overline{d_p}$ = 4.2±0.4 nm particles) and PLE (dashed lines, emission wavelength λ_{em} = 536 nm for 4.2 nm particles and λ_{em} = 476 nm for 3.1 nm particles) spectra of 3.1 and 4.2 nm Ge nanoparticles dispersed in chloroform. The intensity has been normalized for comparison. The PL quantum yields for the 3.1 and 4.2 nm Ge nanocrystals are 6.6% (at 340 nm) and 4.6% (at 360 nm) respectively, determined using a reference solution of quinine bisulfate (quantum yield = 0.55, Sigma-Aldrich) in 0.1 M sulfuric acid. The reported particle diameters were determined from histograms obtained from TEM images of 125 and 86 particles for the 3.1 and 4.2 nm nanocrystals, respectively.

a major peak at 476 nm (2.6 eV) that is blue-shifted relative to the 4.2 nm particles. The observed ∼60 nm blue shift is greater than the difference in excitation wavelength (∼20 nm), indicating that the effect of quantum confinement is likely playing a role in the optical properties of the nanocrystals. However, the Ge nanocrystal PL can be very sensitive to the surface chemistry[27,28] and must be more thoroughly examined in future experimental work to fully understand the nature of the observed size-dependent blue shifts in the absorption and PL spectra.

The window of potential reaction conditions for producing Ge nanocrystals depends sensitively on the Ge precursor chemistry. Significantly lower temperatures and residence times, and higher octanol concentrations, are required when DPG is used (400 °C, 20 s) compared to TEG (450 °C, 5 min). This significant difference relates to the much lower kinetic stability of the Ge−phenyl bond compared to the Ge−alkyl bond.[29] These observations for nanocrystal growth are consistent with our findings for Ge nanowires, in which DPG is a more reactive precursor than TEG, requiring lower temperatures to produce nanowires in supercritical solvents.[11] The greater reactivity of DPG provides a narrower range of conditions that will yield nanometer-size particles, yet enables a broader range of sizes to be produced, simply by varying the precursor concentration.

Although the quality of the nanocrystal product is relatively high, with nanocrystal diameter being tunable over a wide range, from 2.0 to 71 nm, with crystalline cores and in many cases relatively narrow size distributions (<∼10), along with visible photoluminescence with reasonably high quantum yields of 4∼6% (which incidentally is higher than the reported quantum yields of 1.5% for 3.7 nm Ge nanoparticles[3] and 0.5% for 4 nm Ge nanoparticles in a SiO_2 matrix[30]), the yield (or conversion) of Ge reactant to Ge nanocrystals is relatively low. The highest yield was achieved for the 100 mM DPG at 400 °C, which was 6.9%. We found that low precursor concentrations were necessary to form smaller nanocrystals; however, under these conditions the yield decreased significantly. TEG degradation at 100 mM at higher temperature (450 °C) gave a lower reaction yield (<1.0%) than DPG at the same reactant concentration. Yields of this magnitude are simply not scalable to commercial production and must be improved if possible. The relatively low yield of the Ge nanocrystals appears to be due to the many competing molecular and oligomeric side reactions that lead to a high ratio of byproduct to Ge nanocrystals that is difficult to overcome in this reaction system. Improvements in reaction yield using this approach require the identification of more suitable organogermane precursor, organic solvent, and capping ligand combinations. Fundamental calculations accounting for precursor degradation kinetics, capping ligand surface binding interactions, and particle nucleation and growth kinetics would certainly be a useful guide to optimizing this synthetic system.

Acknowledgment. We thank the NSF, DOE, and the Welch Foundation for financial support of this work. The authors also thank J. P. Zhou for assistance with the HRTEM, D. Aherne for XRD and TEM data of polycrystalline Ge formed from TEG decomposition in pure hexane, and L. Pell, T. Hanrath, F. Mikulec, and D. Jurbergs for valuable discussions.

References

(1) *Semiconductor and Metal Nanocrystals: Synthesis, Electronic and Optical Properties*; Klimov, V. I., Ed.; Marcel Dekker: New York, 2003.
(2) Wilcoxon, J. P.; Provencio, P. P.; Samara, G. A. *Phys. Rev. B.* **2001**, *64*, 035417.

(3) Tanke, R. S.; Kauzlarich, S. M.; Patten, T. E.; Pettigrew, K. A.; Murphy, D. L.; Thompson, M. E.; Lee, H. W. H. *Chem. Mater.* **2003**, *15*, 1682.
(4) Heath, J. R.; Shiang, J. J.; Alivisatos, A. P. *J. Chem. Phys.* **1994**, *101*, 1607.
(5) Dutta, A. K. *Appl. Phys. Lett.* **1996**, *68*, 1189.
(6) Wang, D.; Dai, H. *Angew. Chem., Int. Ed.* **2002**, *41*, 4783.
(7) Holmes, J. D.; Ziegler, K. J.; Doty, R. C.; Pell, L. E.; Johnston, K. P.; Korgel, B. A. *J. Am. Chem. Soc.* **2001**, *123*, 3743.
(8) Ziegler, K. J.; Doty, R. C.; Johnston, K. P.; Korgel, B. A. *J. Am. Chem. Soc.* **2001**, *123*, 7797−7803.
(9) Holmes, J. D.; Johnston, K. P.; Doty, R. C.; Korgel, B. A. *Science* **2000**, *287*, 1471.
(10) Lu, X.; Hanrath, T.; Johnston, K. P.; Korgel, B. A. *Nano Lett.* **2003**, *3*, 93.
(11) Hanrath, T.; Korgel, B. A. *J. Am. Chem. Soc.* **2002**, *124*, 1424.
(12) Hanrath, T.; Korgel, B. A. *Adv. Mater.* **2003**, *15*, 437.
(13) Davidson, F. M.; Schricker, A. D.; Wiacek, R. J.; Korgel, B. A. *Adv. Mater.* **2004**, in press.
(14) English, D. S.; Pell, L. E.; Yu, Z.; Barbara, P. F.; Korgel, B. A. *Nano Lett.* **2002**, *2*, 681.
(15) Ding, Z.; Quinn, B. M.; Haram, S. K.; Pell, L. E.; Korgel, B. A.; Bard, A. J. *Science* **2002**, *296*, 1293.
(16) TEM and selected area electron diffraction (SAED) were performed using a JEOL 2010F TEM operating at 200 kV equipped with a GATAN digital photography system. TEM samples were prepared by drop casting nanocrystals from chloroform dispersions onto 200 mesh copper grids with ultrathin carbon film (Ladd Research, VT) or lacy carbon film (Electron Microscopy Sciences, PA). Energy-dispersive X-ray spectroscopy (EDS) was performed on the JEOL 2010F HRTEM equipped with an Oxford spectrometer.
(17) The Ge precursor solution was loaded into a 1 mL titanium grade-2 cell (0.5 cm i.d., 2.0 cm o.d., and 7.0 cm long with a titanium grade-2 LM6 HIP gland and plug, High-Pressure Equipment, Inc) in a nitrogen glovebox. A brass block (7 × 25 × 17 cm) was used to heat the reactor. The block was thermostated with a thermocouple (Omega, Inc.) and a temperature controller, and heated by four 300 W 1/4 in. diameter by 4.5 in. long cartridge heaters (Omega). The block was heated to the desired reaction temperature prior to inserting the cell. The cell was inserted into the preheated block and reached the synthesis temperature in 2 min. The reaction proceeded another 5 min for TEG and 20 s for DPG at this temperature.
(18) Cowley, J. M. *Electron Diffraction Techniques*; Oxford Science University Press: New York, 1992; Vol. 1.
(19) Cullity, B. D. *Elements of X-ray Diffraction*; Addison-Wesley: Reading, MA, 1956.
(20) Inagaki, N.; Mitsuuchi, M. *J. Polym. Sci.* **1983**, *21*, 2887.
(21) Pretsch, E.; Clerc, T.; Seibl, J.; Simon, W. *Tables of Spectral Data for Structure Determination of Organic Compounds*; Springer-Verlag: Berlin, 1983.
(22) Socrates, G. *Infrared Characteristic Group Frequencies: Tables and Charts*; 2nd ed.; John Wiley & Sons: New York, 1994.
(23) Taylor, B. R.; Kauzlarich, S. M.; Delgado, G. R.; Lee, H. W. *Chem. Mater.* **1999**, *11*, 2493.
(24) Melnikov, D. V.; Chelikowsky, J. R. *Solid State Commun.* **2003**, *127*, 361.
(25) Reboredo, F. A.; Zunger, A. *Phys. Rev. B* **2000**, *62*, R2275.
(26) Takagahara, T.; Takeda, K. *Phys. Rev. B* **1996**, *53*, R4205.
(27) Okamoto, S.; Kanemitsu, Y. *Phys. Rev. B* **1996**, *54*, 16421.
(28) Reboredo, F. A.; Zunger, A. *Phys. Rev. B* **2001**, *63*, 235314.
(29) *The Chemistry of Organic Germanium, Tin and Lead Compounds, Volume 2 (Part 1)*; Rappoport, Z., Ed.; John Wiley & Sons: Chichester, England, 2002; Vol. 2.
(30) Kanemitsu, Y.; Uto, H.; Masumoto, Y.; Maeda, Y. *Appl. Phys. Lett.* **1992**, *61*, 2187.

NL049831J